doi: 10.15407/ujpe61.10.0909

M.O. DANILOV,[1] I.A. RUSETSKII,[1] I.A. SLOBODYANYUK,[1] G.I. DOVBESHKO,[2] G.YA. KOLBASOV,[1] YU.YU. STUBROV[3]

[1] Vernadskyi Institute of General and Inorganic Chemistry, Nat. Acad. of Sci. of Ukraine
(32/34, Academician Palladin Ave., Kyiv 03680, Ukraine)
[2] Institute of Physics, Nat. Acad. of Sci. of Ukraine
(46, Prosp. Nauky, Kyiv 03028, Ukraine)
[3] V.E. Lashkaryov Institute of Semiconductor Physics, Nat. Acad. of Sci. of Ukraine
(41, Prosp. Nauky, Kyiv 03028, Ukraine)

SYNTHESIS, PROPERTIES, AND APPLICATION OF GRAPHENE-BASED MATERIALS OBTAINED FROM CARBON NANOTUBES AND ACETYLENE BLACK

PACS 61.48.De, 81.05.ue, 82.45.Fk

Graphene oxide and reduced graphene oxide have been chemically synthesized from multiwall carbon nanotubes. Using a proper oxidant, nanotubes can be "unzipped" longitudinally to form graphene oxide nanoribbons. Afterward, reduced graphene oxide can be obtained with the help of a reductant. Standard redox potentials of carbon are used for the selection of an oxidant and a reductant. Various physico-chemical methods are applied to verify the production of graphene-like materials. The synthesized products are used as a material for oxygen electrodes in fuel elements. The electrochemical characteristics of electrodes fabricated from graphene-based materials are found to depend on the redox ability of applied reagents. The obtained materials are shown to be promising catalyst carriers for electrodes in chemical current sources.

K e y w o r d s: graphene oxide, reduced graphene oxide, electrocatalysis, electrode materials for oxygen electrode.

1. Introduction

The application of the air or oxygen electrodes in devices that generate electric energy is rather promising, because it does not create environmental problems and allows nonrenewable natural resources to be preserved. An air or oxygen electrode in a current source comprises a three-phase electrode–electrolyte–gas system, in which the processes of electric current generation are localized at the phase interfaces. The current generated by this gas diffusion electrode depends on the size of the triple contact between the three indicated phases. The electrode consists of a catalyst and a carrier, and the interaction between those components is the main factor governing the magnitude of generated current.

At present, platinum is the most effective catalyst for the oxygen reduction. However, it possesses an essential shortcoming: this is its high price. There are a tremendous number of works aimed at researching other effective catalysts (see, e.g., work [1]). A catalytically active and stable carrier is the other important problem. In works [2–4], the advantage of using carbon nanotubes as a catalyst carrier was demonstrated. Today, challenging are researches of a new nanocarbon material, graphene, as an electrode material for lithium-ionic accumulators [5] and as a catalyst carrier in fuel elements [6–10].

The following methods that allow graphene to be produced from carbon nanotubes are known: the intercalation of alkaline-earth elements [11, 12] and nitrogen [13]; plasma etching [14–16]; microwave [17, 18], ultrasonic [21, 22], and electrochemical [27] unzipping; catalytic unzipping by metal nanoparticles [19,20]; application of laser radiation [23], electric current [24], and a probe of scanning tunnel microscope [26]; high-temperature hydrogenation [25]; and redox chemical synthesis [28, 29]. The chemical synthesis of graphene-based materials includes a stage of producing graphene oxide (GO) and its subsequent reduction, which gives rise to the so-called reduced graphene oxide (RGO). The synthesis, structure, and chemical properties of graphene oxide and reduced

graphene oxide were classified and described in reviews [28–31] in detail.

The aim of this work consists in the study of the role of oxidants and reductants in the chemical synthesis of graphene materials obtained from multiwall carbon nanotubes and acetylene black, as well as their influence on the electrochemical characteristics of an oxygen electrode fabricated on their basis.

2. Experimental Part

The following reactants of the chemically pure grade were used: H_2SO_4 (98%), HF (40%), HCl (35%), $KMnO_4$, $K_2Cr_2O_7$, $NaH_2PO_2 \cdot H_2O$, Na_2SO_3, H_2PtCl_6, $Pb(CH_3COO)_2 \cdot 3H_2O$, and KOH. Bidistilled water was used for washing the specimens and for the preparation of solutions.

Multiwall carbon nanotubes (MWCNTs) and acetylene black (electrically conducting carbon black of P267E grade) were used as a precursor for the synthesis of graphene-based materials. Carbon nanotubes were obtained with catalytically pyrolyzing acetylene on a catalyst. The external diameter of MWCNTs amounted to about 10–40 nm, the specific surface to 230 m^2/g, the bulk density to 25–30 g/dm^3, and the number of walls varied from 8 to 15. The MWCNTs were cleared of the catalyst remnants by treating in a hydrofluoric acid solution.

Platinum was deposited from an aqueous solution containing 3% of H_2PtCl_6 and 0.2% of lead (II) acetate, by applying the electrolysis at a voltage of ± 1 V for 2 min. In so doing, the current direction was changed every 30 s.

Reduced graphene oxide was synthesized by dispersing 1 g of MWCNTs in 30 ml of H_2SO_4 solution (98%) with the permanent stirring for an hour. Then, 10 g of $K_2Cr_2O_7$ was added, and the mixture was periodically stirred during 72 h. Further, the dispersion was filtered out and, afterward, washed out in a 10% HCl solution and distilled water on a dense filter paper with narrow pores. The product was reduced similarly to the technique described in work [32]. The procedure for obtaining RGO making use of $KMnO_4$ was also described in work [32].

The synthesized RGO materials were applied as an active layer in oxygen electrodes. Two-layer oxygen electrodes were fabricated by pressing. The hydrophobic layer contained 0.07 g/cm^2 of acetylene black and 25% of polytetrafluorethylene, whereas the active layer contained 0.02 g/cm^2 of the synthesized material and 5% of polytetrafluorethylene.

A mockup of fuel element for testing the gas diffusion electrodes was described in work [33]. A zinc electrode was used as an anode. The 6 M KOH solution served as an electrolyte. An U-shaped electrolyzer with an alkaline electrolyte was used as a source of oxygen. Oxygen was supplied to the gas electrodes under an excess pressure of 0.01 MPa. Before the measurements, the oxygen electrode was blown through with oxygen for an hour. A chlorine-silver electrode connected by a salt bridge was a reference one. The load characteristics were registered in the galvanostatic regime.

The obtained RGO specimens were studied on an electron microscope JEM-100 CXII. Raman spectra were registered on a spectrometer T-64000 Horiba Jobin-Yvon. An Ar–Kr ionic laser with an excitation wavelength of 488.0 nm and a power of 2 mW was used in the experiment. The laser radiation was focused onto the specimen by means of a 50x zoom optical lens. The position of the reference specimen (a Si crystal) at 520 cm^{-1} was used as a reference point to calibrate wave numbers. The presence of impurities in the specimens was determined making use of IR spectroscopy in the reflection-absorption mode (the reflection-absorption spectrometry, RAS) on an IFS-66 Bruker spectrometer. The software code Opus 4.2.37 was used to treat and analyze the measured spectra. The frequency reproducibility in the IR spectral range amounted to ± 0.5 cm^{-1} (± 0.0005 cm^{-1} for absorption).

3. Results and Their Discussion

Multiwall carbon nanotubes are characterized by a strained structure of their graphene layers, which results in a reduction of the binding energy between carbon atoms in a graphene layer. Using a suitable strong oxidant, the nanotubes can be longitudinally "unzipped" to form GO nanoribbons. Afterward, by applying a strong reductant to them, RGO can be obtained.

Proceeding from the standard redox potentials of carbon [34] (see Table 1), oxidants with potentials more electropositive than +0.528 V have to be applied for the oxidation of carbon in an acid medium. We may assume that, to oxidate carbon in

an alkaline medium, a potential more electropositive than −0.603 V is required.

The most known strong oxidants (acid/alkaline medium) are $KMnO_4$ (+1.69 V/+0.588 V), O_3 (+2.075 V/+1.247 V), $Cr_2O_7^{2-}$ (+1.36 V/no data), OsO_4 (+1.02 V/+0.17 V), FeO_4^{2-} (+2.07 V/+0.8 V), and some others [34]. However, if the rupture of bonds between carbon atoms in nanotubes is caused by kinetic restrictions, the thermodynamic redox scale for this process cannot be applied. Accordingly, in order to reduce GO in an alkaline or acid medium, reductants with potentials more electronegative than −1.148 or −0.320 V, respectively, are required. To oxidize MWCNTs in an acid medium, the $KMnO_4$ (+1.69 V) and $K_2Cr_2O_7$ (+1.36 V) were used. The solutions of sodium hypophosphite (−1.51 V) and sodium sulfite (−0.936 V) in an alkaline medium [34] were used as reductants.

Micrographs of RGO reduced from GO with the help of sodium sulfite and sodium hypophosphite can be found in work [32]. GO was obtained by oxidizing MWCNTs, by taking advantage of potassium permanganate.

The X-ray diffraction analysis [35] revealed the presence of two spectral peaks. One of them is located at the angle $2\theta = 25.6°$ and corresponds to a reflex from the interplane distance between the graphene layers. The other is located in a vicinity of the angle $2\theta = 21°$ and corresponds to SiO_2. The distance between planes in graphene turns out to be equal to 3.43 Å, which is larger than the corresponding distance in graphite (3.35 Å). The initial nanotubes and the synthesized RGO specimens had similar reflexes, but, in the RGO case, the right reflex ($2\theta = 25.6°$) became wider, and the specimen crystallinity worsened after the treatment, which testifies to a decrease of particle dimensions [35].

In Fig. 1, comparative current-voltage characteristics of oxygen electrodes on the basis of RGO (curves *2* to *4*), as well as electrodes on the basis of initial MWCNTs (curve *1*) and MWCNTs with deposited metallic platinum (10 wt.%) (curve *5*) are depicted. Curve *2* characterizes the electrode fabricated on the basis of RGO obtained from carbon nanotubes oxidized by potassium permanganate and afterward reduced by sodium sulfite (S–RGO–Mn). Curve *3* corresponds to the electrode on the basis of RGO obtained from carbon nanotubes oxidized by potassium bichromate and afterward reduced by sodium hypophosphite (H–RGO–Cr). Finally, curve *4* is a characteristic of the electrode on the basis of RGO obtained from carbon nanotubes oxidized by potassium permanganate and afterward reduced by sodium hypophosphite (H–RGO–Mn). The presented current-voltage curves testify that the current efficiency of oxygen electrodes on the basis of H–RGO–Mn is higher than that of electrodes on the basis of H–RGO–Cr. This fact confirms that the load characteristics depend on the oxidizing capability of used oxidants.

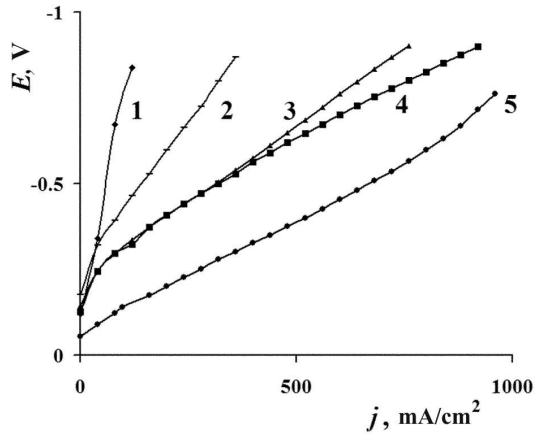

Fig. 1. Load characteristics of oxygen electrodes with various active layers: initial MWCNTs (*1*), S–RGO–Mn (*2*), H–RGO–Cr (*3*), H–RGO–Mn (*4*), and MWCNTs with 10 wt.% of Pt (*5*)

The oxidation of MWCNTs was shown to give rise to essential changes in the structure of graphene oxide, if potassium permanganate was applied. Namely, the number of structural defects increased, the nanotube unzipping became better, the number of

Table 1. **Standard electrode redox potentials E^0 for carbon**

Acid medium E^0, V		Alkaline medium E^0, V	
Oxidation			
C, H^+/CH_3OH	−0.32 V	C/CH_3OH, OH^-	−1.48 V
C, H^+/CH_3OH	+0.528 V	CHO^{2-}/C, OH^-	−0.603 V
CO, H^+/C	+0.518 V	CO_3^{2-}/C, OH^-	−0.766 V
H_2CO_3, H^+/C	+0.207 V		
Reduction			
C, H^+/CH_3OH	−0.320 V	C/CH_3OH, OH^-	−1.148 V
$HCHO_2$, H^+/C	+0.528 V	CHO^{2-}/C, OH^-	−0.603 V
H_2CO_3, H^+/C	+0.27 V	CO_3^{2-}/C, OH^-	−0.766 V

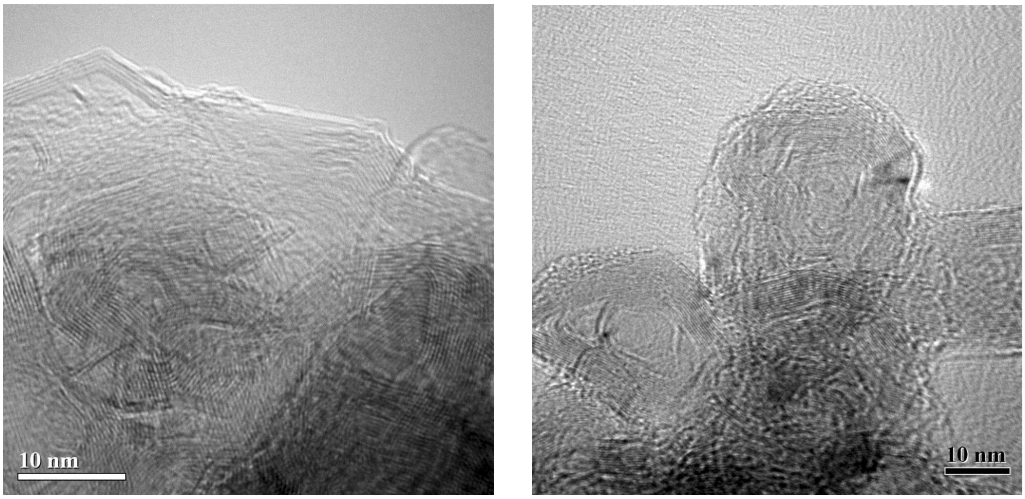

a *b*

Fig. 2. Micrographs of specimens: (*a*) acetylene black and (*b*) RGO obtained from acetylene black oxidized by $K_2Cr_2O_7$ and reduced by sodium hypophosphite

graphene layers diminished in comparison with that in initial nanotubes, and the dimensions of particles decreased. In the case of oxidation with the use of $K_2Cr_2O_7$, the number of graphene layers slightly decreased or remained the same as in carbon nanotubes [35].

It should be noted that the current density at the oxygen electrodes also depends on the reducing ability of applied reductants. The standard redox potential of sodium sulfite in the alkaline medium ($E^0 = -0.936$ V) is more positive than that of sodium hyposulfite ($E^0 = -1.51$ V), which testifies to its lower reducing ability. In particular, provided the same polarization, the load characteristics for the electrode on the basis of H–RGO–Mn (Fig. 1, curve *4*) are located above those for the electrode on the basis of S–RGO–Mn (Fig. 1, curve *2*). We assume [35] that sodium sulfite partially reduces some carboxy groups, because the required reduction potential for GO should be more electronegative, $E^0 = -1.148$ V [34].

As one can see from Fig. *1*, the current efficiency of the electrodes on the basis of H–RGO–Mn (curve *4*) is close to that of the electrodes on the basis of platinum-containing materials (curve *5*). This fact testifies that they are promising to be used as cathode materials for oxygen electrodes in fuel elements.

We also oxidized acetylene black by means of $K_2Cr_2O_7$ and reduced the obtained product, by using sodium hyposulfite. The oxidation-reduction method for acetylene black was analogous to that described above. In Fig. 2, micrographs of initial acetylene black (panel *a*) and RGO obtained from it (panel *b*) are depicted.

Acetylene black is composed of granules consisting of multiwall graphene particles (Fig. 2, *a*) that are connected chaotically and closely with one another by means of covalent and non-covalent (van der Waals) forces. After the oxidation by potassium bichromate and the reduction by sodium hyposulfite, these granules became separated into individual particles, each of them consisting of tens of graphene layers (see Fig. 2, *b*).

With the help of Raman scattering spectroscopy (Fig. 3), a good crystallinity of the obtained specimens of a graphene-like material was proved; namely, the presence of G (1587 cm^{-1}) and D (1361 cm^{-1}) modes [36], which became narrower at the chemical treatment of acetylene black, and its transformation into graphite particles. The band at 1587 cm^{-1} got narrower from 66 cm^{-1} in acetylene black to 37 cm^{-1} in RGO, and the band at 1361 cm^{-1} from 190 to 50 cm^{-1} [37]. The location of the G-mode at 1587 cm^{-1} testified that the particles were in the strained state, and then they coagulated into globules. There were no overtones in the acetylene black spectrum. This fact confirms a disordered arrangement of the blocks of the initial material. The spec-

trum of acetylene black was similar to that of pyrocarbon, so that the structure and the properties of those specimens may also be similar [38].

After the treatment, there appeared overtones at 2713, 2949, and 3239 cm^{-1}, which testifies to the crystallinity of the obtained material. The IR spectroscopy method (Fig. 4) revealed an insignificant amount of impurities in it. The analysis of IR spectra allows us to draw a conclusion that all specimens – initial, after the oxidation, and after the reduction – contain C–C and C–O (a spectral interval of 950–1300 cm^{-1}), C=O and C=C (1480–1650 cm^{-1}), and OH (3410–3460 cm^{-1}) molecular groups. Some bands below 900 cm^{-1} are associated with collective-mode vibrations with the participation of CC bonds of several graphene rings with dangling ends. Probably, they can be characteristic of graphite-containing materials like thermally expanded graphite, carbon nanotubes, and fullerenes [39, 40]. The manifestation of those low-frequency vibrations in the IR interval testifies to the presence of dangling bonds. The amount of impurities in all specimens was insignificant and remained almost constant at their treatment. Nevertheless, a bit more impurities were observed in the initial material; namely, after the oxidation, the traces of CH in an interval of 2800–3000 cm^{-1} became a little more intense than the band at 1380–1650 cm^{-1}.

Figure 5 demonstrates the current-voltage dependences of oxygen electrodes on the basis of graphene-like materials obtained from acetylene black. One can see that the electrodes from oxidized acetylene black (curve *2*) have better parameters than initial carbon black. In our opinion, a small deterioration of the load characteristics of oxygen electrodes fabricated from graphene-like materials in the current density interval below 100 mA/cm^2 is associated with the fact that, at such current densities, oxygen adsorbed on the surface of acetylene black makes a contribution to the oxygen reduction reaction, which increases the current generated at the electrode.

Electrodes from RGO obtained from acetylene black demonstrated better characteristics in comparison with electrodes from GO obtained by oxidizing acetylene black (Fig. 5, curve *3*). This result can be explained by the fact that the oxidant on the basis of potassium bichromate did not allow us to obtain completely oxidized graphene oxide.

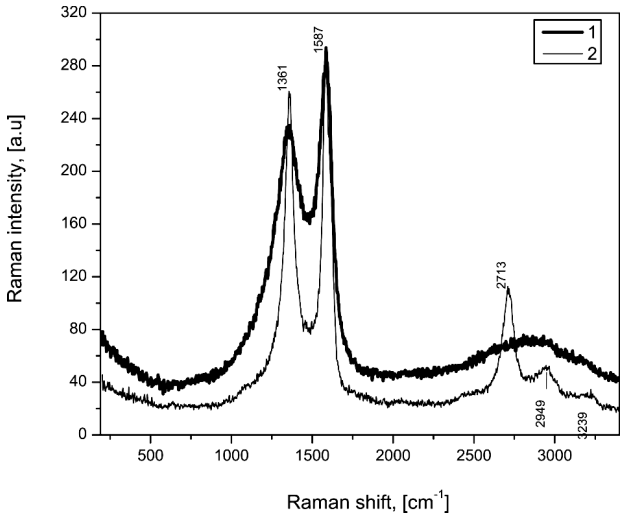

Fig. 3. Raman spectra obtained at 488 nm for initial acetylene black (*1*) and RGO obtained from acetylene black oxidized by $K_2Cr_2O_7$ and reduced by sodium hypophosphite (*2*)

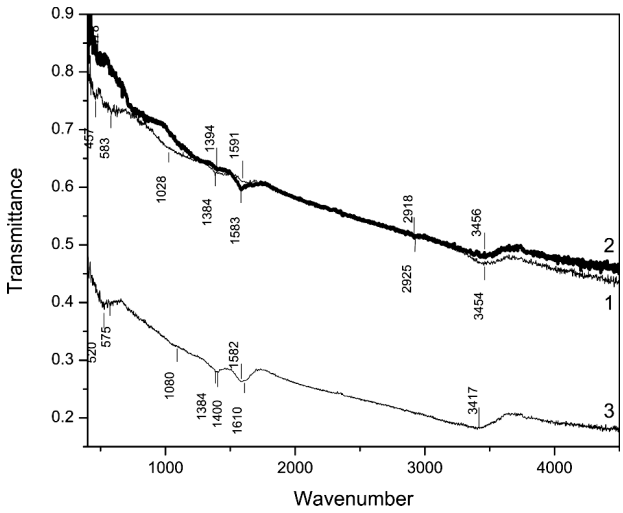

Fig. 4. IR spectra for initial acetylene black (*1*), acetylene black oxidized by $K_2Cr_2O_7$ (*3*), and acetylene black obtained from acetylene black oxidized by $K_2Cr_2O_7$ and reduced by sodium hypophosphite (*2*)

For the electrode from GO doped with sulfur and nitrogen, the specific capacitance equals 415 mA h/g [41]. At the same time, for the oxygen electrode on the basis of RGO doped with nitrogen and with deposited $LiMn_2O_4$, the specific capacitance equals 585 mA h/g [42]. The specific capacitance calculated for our electrode under the same conditions turned out to approximately equal 500 mA h/g. Hence, the

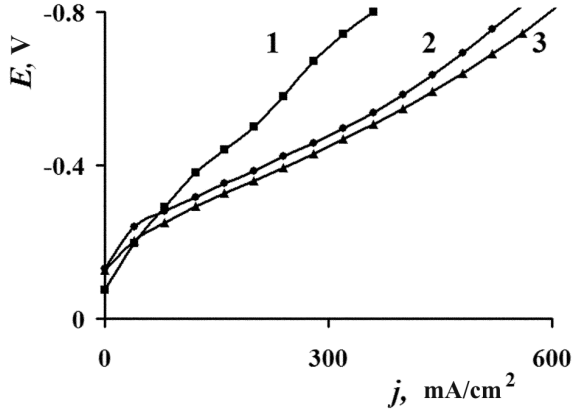

Fig. 5. Potential dependence on the current density for oxygen electrodes with an active layer (0.02 g/ cm^{-2}) consisting of initial acetylene black (*1*), acetylene black oxidized by potassium bichromate (*2*), and RGO reduced by sodium hyposulfite from acetylene black oxidized by potassium bichromate (*3*)

proposed simplified technique aimed at producing the specimens of oxidized and reduced graphene makes it possible to obtain materials for catalyst carriers that are not worse than their foreign analogs.

All examined graphene materials were stable within six months when being tested in the galvanostatic regime in the fuel-element mockup at a current density of 200 mA/ cm^{-2} at oxygen electrodes.

4. Conclusions

It was found that, using the standard redox potential scale, suitable oxidants and reductants for the synthesis of reduced graphene oxide from multiwall carbon nanotubes and acetylene black can be chosen. The obtained graphene-like materials are shown to be promising as catalyst carriers for oxygen electrodes in fuel elements. In particular, they can substitute commercial electrode materials that contain platinum.

1. F. Bidault, D.J.L. Brett, P.H. Middleton *et al.,* Review of gas diffusion cathodes for alkaline fuel cells, *J. Power Sourc.* **187**, 39 (2009) [DOI: 10.1016/j.jpowsour.2008.10.106].
2. M. Soehn, M. Lebert, T. Wirth *et al.,* Design of gas diffusion electrodes using nanocarbon, *J. Power Sourc.* **176**, 494 (2008) [DOI: 10.1016/j.jpowsour.2007.08.073].
3. C-T. Hsieh, J-Yi. Lin, and J.-L. Wei, Deposition and electrochemical activity of Pt-based bimetallic nanocatalysts on carbon nanotube electrodes, *Int. J. Hydrogen Energy* **34**, 685 (2009) [DOI: 10.1016/j.ijhydene.2008.11.008].
4. X. Wang, M. Waje, and Y. Yan, NT-based electrodes with high efficiency for PEMFCs, *Electrochem. Solid-State Lett.* **8**, A42 (2005) [DOI: 10.1149/1.1830397].
5. G. Wang, X. Shen, J. Yao *et al.,* Graphene nanosheets for enhanced lithium storage in lithium ion batteries, *Carbon* **47**, 2049 (2009) [DOI: 10.1016/j.carbon.2009.03.053].
6. Y. Xin, J. Liu, X. Jie *et al.,* Preparation and electrochemical characterization of nitrogen doped graphene by microwave as supporting materials for fuel cell catalysts, *Electrochim. Acta* **60**, 354 (2012) [DOI: 10.1016/j.electacta.2011.11.062].
7. Z. Lin, G. Waller, Y. Liu *et al.,* Facile synthesis of nitrogen-doped graphene via pyrolysis of graphene oxide and urea, and its electrocatalytic activity toward the oxygen-reduction reaction, *Adv. Energy Mater.* **2**, 884 (2012) [DOI: 10.1002/aenm.201200038].
8. L.T. Qu, Y. Liu, J.B. Baek *et al.,* Nitrogen-doped graphene as efficient metal-free electrocatalyst for oxygen reduction in fuel cells, *ACS Nano* **4**, 1321 (2010) [DOI: 10.1021/nn901850u].
9. Z.Y. Lin, M.K. Song, Y. Ding *et al.,* Facile preparation of nitrogen-doped graphene as a metal-free catalyst for oxygen reduction reaction, *Phys. Chem. Chem. Phys.* **14**, 3381 (2012) [DOI: 10.1039/C2CP00032F].
10. Y. Shao, S. Zhang, C. Wang *et al.,* Highly durable graphene nanoplatelets supported Pt nanocatalysts for oxygen reduction, *J. Power Sourc.* **195**, 4600 (2010) [DOI: 10.1016/j.jpowsour.2010.02.044].
11. A.G. Cano-Márquez, F.J. Rodríguez-Macías, J. Campos-Delgado *et al.,* Ex-MWNTs: Graphene sheets and ribbons produced by lithium intercalation and exfoliation of carbon nanotubes, *Nano Lett.* **9**, 1527 (2009) [DOI: 10.1021/nl803585s].
12. D.V. Kosynkin, W. Lu, A. Sinitskii *et al.,* Highly conductive graphene nanoribbons by longitudinal splitting of carbon nanotubes using potassium vapor, *ACS Nano* **5**, 968 (2011) [DOI: 10.1021/nn102326c].
13. A. Morelos-Gómez, S.M. Vega-Díaz, V.J. González *et al.,* Clean nanotube unzipping by abrupt thermal expansion of molecular nitrogen: Graphene nanoribbons with atomically smooth edges *ACS Nano* **6**, 2261 (2012) [DOI: 10.1021/nn2043252].
14. L. Jiao, L. Zhang, X. Wang *et al.,* Narrow graphene nanoribbons from carbon nanotubes, *Nature* **458**, 877 (2009) [DOI: 10.1038/nature07919].
15. L. Valentini, Formation of unzipped carbon nanotubes by CF4 plasma treatment, *Diamond Rel. Mater.* **20**, 445 (2011) [DOI: 10.1016/j.diamond.2011.01.038].
16. S. Mohammadi, Z. Kolahdouz, S. Darbari *et al.,* Graphene formation by unzipping carbon nanotubes using a sequential plasma assisted processing, *Carbon* **52**, 451 (2013) [DOI: 10.1016/j.carbon.2012.09.056].
17. I. Janowska, O. Ersen, T. Jacob *et al.,* Catalytic unzipping of carbon nanotubes to few-layer graphene sheets under mi-

crowaves irradiation, *Appl. Catal. A* **371**, 22 (2009) [DOI: 10.1016/j.apcata.2009.09.013].
18. S. Vadahanambi, J-H. Jung, R. Kumar *et al.,* An ionic liquid-assisted method for splitting carbon nanotubes to produce graphene nano-ribbons by microwave radiation, *Carbon* **53**, 391 (2013) [DOI: 10.1016/j.carbon.2012.11.029].
19. A.L. Elías, As.R. Botello-Méndez, D. Meneses-Rodríguez *et al.,* Longitudinal cutting of pure and doped carbon nanotubes to form graphitic nanoribbons using metal clusters as nanoscalpels, *Nano Lett.* **10**, 366 (2009) [DOI: 10.1021/nl901631z].
20. U.K. Parashar, S. Bhandari, R.K. Srivastava *et al.,* Single step synthesis of graphene nanoribbons by catalyst particle size dependent cutting of multiwalled carbon nanotubes, *Nanoscale* **3**, 3876 (2011) [DOI: 10.1039/C1NR10483G].
21. L. Jiao, X. Wang, G. Diankov *et al.,* Facile synthesis of high-quality graphene nanoribbons, *Nat. Nanotechnol.* **5**, 321 (2010) [DOI: 10.1038/nnano.2010.54].
22. L. Xie, H. Wang, C. Jin *et al.,* Graphene nanoribbons from unzipped carbon nanotubes: Atomic structures, Raman spectroscopy, and electrical properties, *J. Am. Chem. Soc.* **133**, 10394 (2011) [DOI: 10.1021/ja203860a].
23. P. Kumar, L.S. Panchakarla, and C.N.R. Rao, Laser-induced unzipping of carbon nanotubes to yield graphene nanoribbons, *Nanoscale* **3**, 2127 (2011) [DOI: 10.1039/C1NR10137D].
24. K. Kim, A. Sussman, and A. Zettl, Graphene nanoribbons obtained by electrically unwrapping carbon nanotubes, *ACS Nano* **4**, 1362 (2010) [DOI: 10.1021/nn901782g].
25. A.V. Talyzin, S. Luzan, I.V. Anoshkin *et al.,* Hydrogenation, purification, and unzipping of carbon nanotubes by reaction with molecular hydrogen: road to graphene nanoribbons, *ACS Nano* **5**, 5132 (2011) [DOI: 10.1021/nn201224k].
26. M.C. Pavia, W. Xu, M.F. Proença *et al.,* Unzipping of functionalized multiwall carbon nanotubes induced by STM, *Nano Lett.* **10**, 1764 (2010) [DOI: 10.1021/nl100240n].
27. D.B. Shinde, J. Debgupta, A. Kushwaha *et al.,* Electrochemical unzipping of multiwalled carbon nanotubes for facile synthesis of high-quality graphene nanoribbons, *J. Am. Chem. Soc.* **133**, 4168 (2011) [DOI: 10.1021/ja1101739].
28. D.V. Kosynkin, A.L. Higginbotham, A. Sinitskii *et al., Nature* **458**, 872 (2009).
29. S. Zhang, L. Zhu, H. Song *et al.,* How graphene is exfoliated from graphitic materials: synergistic effect of oxidation and intercalation processes in open, semi-closed, and closed carbon systems, *J. Mater. Chem.* **22**, 22150 (2012) [DOI: 10.1039/C2JM35139K].
30. Y. Zhu, S. Murali, W. Cai *et al.,* Graphene and graphene oxide: synthesis, properties, and applications, *Adv. Mater.* **22**, 3906 (2010) [DOI: 10.1002/adma.201001068].
31. S. Pei and H.-M. Cheng, The reduction of graphene oxide, *Carbon* **50**, 3210 (2012) [DOI: 10.1016/j.carbon.2011.11.010].
32. M.O. Danilov, I.A. Slobodyanyuk, I.A. Rusetskii *et al.,* Reduced graphene oxide: a promising electrode material for oxygen electrodes, *J. Nanostruct. Chem.* **3**, 1 (2013) [DOI: 10.1186/2193-8865-3-49].
33. M.O. Danilov, G.Ya. Kolbasov, I.A. Rusetskii *et al.,* Electrocatalytic properties of multiwalled carbon nanotubes-based nanocomposites for oxygen electrodes, *Russ. J. Appl. Chem.* **85**, 1536 (2012) [DOI: 10.1134/S1070427212100084].
34. S.G. Bratsch, Standard electrode potentials and temperature coefficients in water at 298.15 K, *J. Phys. Chem.* **18**, 1 (1989) [DOI: 10.1063/1.555839].
35. M.O. Danilov, I.A. Slobodyanyuk, I.A. Rusetskii *et al.,* Influence of the synthesis conditions of reduced graphene oxide on the electrochemical characteristics of the oxygen electrode, *Nanosci. Nanotech. Res.* **2**, 12 (2014) [DOI: 10.12691/nnr-2-1-3].
36. T. Lebedieva, V. Gubanov, G. Dovbeshko, and D. Pidhirnyi, Quantum-chemical calculation and visualization of the vibrational modes of graphene at different points of the Brillouin zone, *Nanoscale Res. Lett.* **10**, 287 (2015) [DOI: 10.1186/s11671-015-0945-9].
37. K. Batrakov, P. Kuzhir, S. Maksimenko, A. Paddubskaya, S. Voronovich, T. Kaplas *et al.,* Enhanced microwave shielding effectiveness of ultrathin pyrolytic carbon films, *Appl. Phys. Lett.* **103**, 073117 (2013) [DOI: 10.1063/1.4818680].
38. G.I. Dovbeshko, V.R. Romanyuk, D.V. Pidgirnyi, V.V. Cherepanov, E.O. Andreev, V.M. Levin, P.P. Kuzhir, T. Kaplas, and Yu.P. Svirko, Optical properties of pyrolytic carbon films versus graphite and graphene, *Nanoscale Res. Lett.* **10**, 234 (2015) [DOI: 10.1186/s11671-015-0946-8].
39. G.I. Dovbeshko, O.P. Gnatyuk, A.A. Nazarova, Yu.I. Sementsov, and E.D. Obraztsova, Conformation analysis of nucleic acids and proteins adsorbed on single-shell carbon nanotubes, *Fulleren. Nanotub. Carbon Nanostr.* **13**, 393 (2005) [DOI: 10.1007/s10947-009-0142-8].
40. S.Ya. Brichka, G.P. Prikhod'ko, Yu.I. Sementsov, A.V. Brichka, O.P. Paschuk, and G.I. Dovbeshko, Synthesis of carbon nanotubes from a chlorine-containing precursor and their properties, *Carbon* **42**, 2581 (2004) [DOI: 10.1016/j.carbon.2004.05.040].
41. P. Ganesan, P. Ramakrishnan, M. Prabu *et al.,* Nitrogen and sulfur co-doped graphene supported cobalt sulfide nanoparticles as an efficient air cathode for zinc-air battery, *Electrochim. Acta.* **183**, 63 (2015) [DOI: 10.1016/j.electacta.2015.05.182].
42. Y. Liu, J. Li, W. Li *et al.,* Spinel $LiMn_2O_4$ nanoparticles dispersed on nitrogen-doped reduced graphene oxide nanosheets as an efficient electrocatalyst for aluminium-air battery, *Int. J. Hydrogen Energy* **40**, 9225 (2015) [DOI: 10.1016/j.ijhydene.2015.05.153].

Received 05.04.16.
Translated from Ukrainian by O.I. Voitenko

М.О. Данилов, І.А. Русецький, І.О. Слободянюк, Г.І. Довбешко, Г.Я. Колбасов, Ю.Ю. Стубров

СИНТЕЗ, ВЛАСТИВОСТІ
ТА ЗАСТОСУВАННЯ ГРАФЕНОВИХ МАТЕРІАЛІВ,
ОТРИМАНИХ З ВУГЛЕЦЕВИХ НАНОТРУБОК
І АЦЕТИЛЕНОВОЇ САЖІ

Р е з ю м е

З багатошарових вуглецевих нанотрубок та ацетиленової сажі були синтезовані оксид графену і відновлений оксид графену. Застосовуючи відповідний окислювач, можна поздовжньо "розгорнути" нанотрубки з утворенням наностріпчок оксиду графену, а потім, впливаючи відновником, отримати відновлений оксид графену. Для вибору окислювача і відновника використані стандартні окислювально-відновні потенціали вуглецю. Різними фізико-хімічними методами було доведено отримання графеноподібних матеріалів. Синтезовані продукти використані в ролі електродного матеріалу для кисневих електродів паливних джерел струму. Встановлено, що електрохімічні характеристики електродів з графенових матеріалів залежать від окислювально-відновної здатності реагентів. Показано, що отримані матеріали є перспективними носіями каталізаторів для електродів хімічних джерел струму.